

## Copper-on-copper homoepitaxy studied by infrared spectroscopy of adsorbed CO

Michael Hancock, Casey Fein, and R. G. Tobin<sup>a)</sup>

*Department of Physics and Astronomy, Tufts University, Medford, Massachusetts 02155, USA*

(Received 27 July 2010; accepted 29 September 2010; published online 25 October 2010)

Infrared spectroscopy of adsorbed CO was used to characterize the dependence of surface structure on deposition temperature during homoepitaxial growth on Cu(100). Intensity borrowing due to dipole coupling greatly enhances the absorption signal due to defect-bonded CO, making it possible to detect and quantify defect concentrations at the level of a few percent. For deposition temperatures between 300 and 400 K, the defect density increases slightly with decreasing deposition temperature but remains below 2%. There is a sharp increase in defect density, up to 5%–6%, as the deposition temperature is decreased from 300 to 250 K. At lower deposition temperatures, there is some sign of a leveling off in defect density, but the IR absorption spectrum becomes so broad that meaningful analysis becomes impractical, while visible degradation of the low-energy electron diffraction pattern indicates worsening surface order. No indication of “re-entrant” ordering at low temperatures was observed for deposition temperatures down to 150 K. © 2010 American Institute of Physics. [doi:10.1063/1.3503970]

### I. INTRODUCTION

It has long been understood that the infrared spectra of adsorbed molecules are strongly affected by dipole-dipole coupling.<sup>1–5</sup> In a homogeneous layer, the consequences include a nonlinear dependence of the absorbance on surface coverage and an upward shift in resonant frequency as the coverage increases. When two species with similar resonant frequencies are coadsorbed, there are additional effects: a downward shift of the lower-frequency mode and an upward shift of the higher-frequency mode, and “intensity borrowing” from the lower- to the higher-frequency mode. Intensity borrowing can lead to the higher-frequency spectral line containing a much greater fraction of the total spectral intensity than the fraction of adsorbates of the corresponding species. In the case of CO adsorption on Cu(100), for example, the C=O vibrational mode associated with CO on defect sites is at higher frequency than that of CO at sites on the flat terraces. As a result, on a surface with a 7% step concentration, the integrated intensity of the absorption peak associated with step CO was shown to be three times greater than that due to the 93% concentration of terrace CO.<sup>6</sup>

We have exploited this hypersensitivity of CO’s infrared spectrum to small defect concentrations to probe the surface quality of copper films grown epitaxially on a Cu(100) surface as a function of the substrate temperature during deposition. Homoepitaxial growth has been extensively studied as a testing ground for understanding fundamental mechanisms of film growth. Since complications such as lattice mismatch, strain, interfacial energies, or differences in surface energy are absent, it is clear that the thermal equilibrium

structure is an atomically flat epitaxial film. Nevertheless, a wide range of nonequilibrium structures are observed, driven by the complex growth kinetics. Evans, Thiel, and Bartelt<sup>7</sup> surveyed recent progress in the field.

Since thermally activated surface diffusion is crucial in determining surface structure, the surface temperature during deposition is a key parameter in determining the smoothness and uniformity of the surface. Previous studies of Cu on Cu homoepitaxy using reflection high-energy electron diffraction (RHEED), He atom scattering, and x-ray scattering have given surprising and not always consistent results. Intensity oscillations in RHEED and He diffraction have been observed at temperatures as low as 100 K, implying layer-by-layer growth even though Cu atoms have negligible mobility at such low temperatures,<sup>8,9</sup> and with some indications that surface roughness actually decreased as the temperature was lowered from 200 to ~160 K.<sup>10</sup> An x-ray scattering study, however, showed the mean-square roughness increasing monotonically with decreasing temperature down to ~150 K, but with markedly smoother growth at 110 K associated with highly strained films with high vacancy concentrations.<sup>11</sup>

Infrared spectroscopy of adsorbed CO, because of its high sensitivity to very low concentrations of surface defects, provides a probe of surface quality that is complementary to the diffraction and scattering methods used previously. We find that small but detectable concentrations of defects appear at deposition temperatures below 400 K, but that the defect concentration increases sharply between 300 and 250 K. We see no evidence of any decrease in defect concentration as the temperature is decreased further to 150 K. Our experiment did not include deposition temperatures lower than 150 K.

<sup>a)</sup>Author to whom correspondence should be addressed. Electronic mail: roger.tobin@tufts.edu.

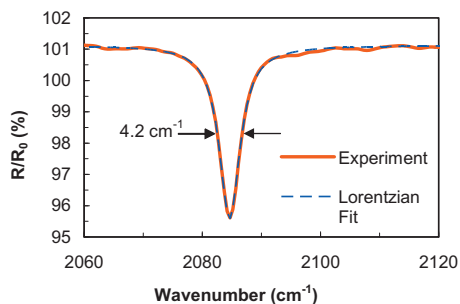


FIG. 1. IR spectrum of a saturation coverage of CO adsorbed onto the clean Cu(100) crystal. A Lorentzian fit to the data is also shown. The experimental linewidth (FWHM) is  $4.2 \text{ cm}^{-1}$ . Correcting for the instrumental resolution of  $2.0 \text{ cm}^{-1}$  gives an inherent linewidth of  $3.7 \text{ cm}^{-1}$ .

## II. EXPERIMENTAL PROCEDURE

The substrate was a Cu(100) single crystal. Prior to installation in the ultrahigh vacuum chamber (base pressure  $<10^{-10}$  Torr), it was electropolished in 80% orthophosphoric acid at a current of  $\sim 0.04 \text{ A/cm}^2$  for 2 min.<sup>12,13</sup> It was then cleaned *in situ* using cycles of Ar<sup>+</sup> sputtering at 500 K and 5 min annealing at 800 K. Surface cleanliness and order were verified with Auger electron spectroscopy and low-energy electron diffraction (LEED). An even more sensitive measure of surface quality, however, is the linewidth of the C=O stretch vibration of adsorbed CO. Linewidths full width at half-maximum (FWHM) of  $4.5 \text{ cm}^{-1}$  or less are indicative of a very smooth, well-ordered surface.<sup>5,14,15</sup> Linewidths of  $6 \text{ cm}^{-1}$  or even greater can often be observed from surfaces that show no detectable contamination in the Auger spectrum and give sharp LEED patterns. We routinely checked the linewidth of CO adsorbed on the Cu(100) substrate before depositing Cu and obtained linewidths of  $4.5 \text{ cm}^{-1}$  or less (average FWHM  $4.35 \pm 0.06 \text{ cm}^{-1}$ ). A typical spectrum, with Lorentzian fit, is shown in Fig. 1. For this spectrum, the measured linewidth was  $4.2 \text{ cm}^{-1}$ . Correcting for the instrumental resolution gives an inherent linewidth of  $3.7 \text{ cm}^{-1}$ . From time to time, after a number of deposition experiments, we would be unable to obtain sufficiently sharp lines merely by sputtering and annealing. The sample would then be removed from the chamber and electropolished. After UHV cleaning, the linewidth would then return to  $<4.5 \text{ cm}^{-1}$ .

For each experiment, a 1.0 nm thick copper film was deposited onto the sample by thermal evaporation from a well-outgassed copper-wrapped tungsten filament at a rate of approximately  $0.002 \text{ nm/s}$ . The thickness and deposition rate were monitored using a quartz crystal thickness monitor. During deposition, the temperature of the sample was held constant within  $\pm 1 \text{ K}$  using liquid-nitrogen cooling and a combination of radiative and electron beam heating controlled by a proportional integral derivative temperature controller. Below 300 K, manual control was used, and the temperature was stable within  $\pm 5 \text{ K}$ .

## III. RESULTS AND DISCUSSION

Following deposition of the Cu film, the sample was cooled to 150 K for CO adsorption by background dosing.

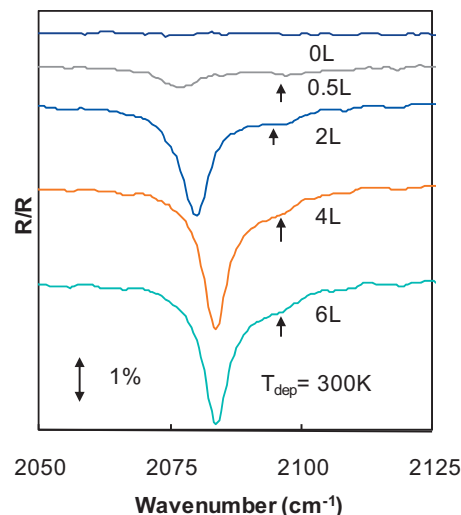


FIG. 2. IR spectra of CO adsorbed onto a Cu film deposited at 300 K for various CO exposures. Curves offset for clarity. As more CO is adsorbed, the secondary feature, indicated by arrows, becomes less noticeable.

Reflection-absorption infrared spectra were measured with unpolarized light at  $86^\circ$  incidence and  $2 \text{ cm}^{-1}$  resolution using a liquid-nitrogen-cooled HgCdTe detector. Figure 2 shows a series of IR spectra for CO adsorption on a Cu film deposited at a substrate temperature of 300 K, for doses from 0 to 6 L (Langmuir:  $1 \text{ L} = 10^{-6} \text{ Torr s}$ ).

The spectrum is dominated by a strong, sharp line near  $2085 \text{ cm}^{-1}$  that is a characteristic of adsorption on the flat Cu(100) surface.<sup>5,6,14-16</sup> In addition, a conspicuous shoulder is visible, especially in the 2 L spectrum, at  $\sim 2095 \text{ cm}^{-1}$ . This feature has been associated with CO adsorbed on atomic-scale defects, such as steps.<sup>5,6</sup>

At lower sample deposition temperatures, the shoulder becomes more prominent and emerges as a distinct secondary peak. Figure 3 shows IR spectra at saturation CO coverage for a range of deposition temperatures from 150 to 400

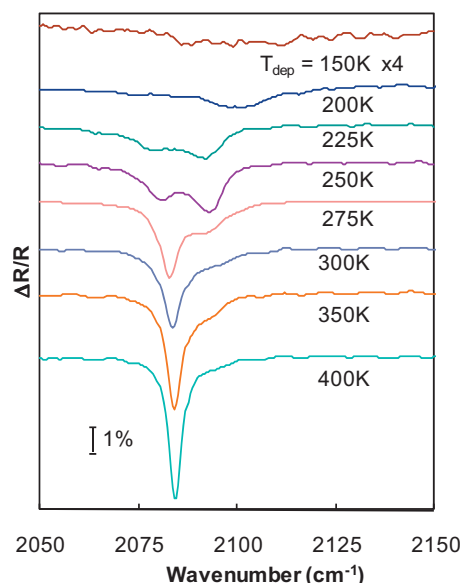


FIG. 3. IR spectra of a saturation coverage of CO on Cu films, for various deposition temperatures. Shouldering and broadening become more pronounced as the deposition temperature is lowered. Spectra offset for clarity.

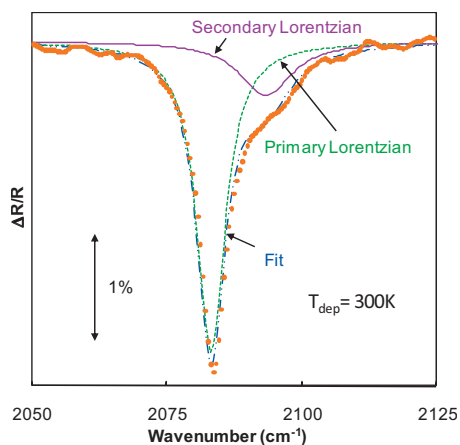


FIG. 4. Example of phenomenological line fitting with two Lorentzian functions. Data are for saturation coverage of CO on a film deposited at 300 K.

K. For a deposition temperature of 400 K, the spectrum is nearly indistinguishable from that of CO on a clean, well-ordered Cu(100) single crystal, consistent with previous results, indicating that at this temperature, Cu atoms diffuse rapidly, and film growth occurs by step propagation.<sup>9</sup> The spectrum for 400 K deposition shows a slight asymmetry that may be due to a small defect concentration not present on the single-crystal surface, but the linewidth is as narrow as for adsorption on the clean single crystal. The increase in intensity of the 2095  $\text{cm}^{-1}$  feature as the deposition temperature is lowered suggests an increasing concentration of atomic-scale structural defects. For deposition temperatures below 225 K, the high-frequency feature broadens and shifts to higher frequency, and no clear peak associated with adsorption on the flat terraces is visible. It is possible that these changes at low temperature are associated with the growth of three-dimensional pyramidal mounds.<sup>10,17</sup>

To quantify the relative intensities of the two peaks, we modeled the saturated spectra phenomenologically as a sum of two Lorentzian functions. Figure 4 shows a typical fit for a saturation coverage of CO on a Cu film deposited at a temperature of 300 K, and Fig. 5 shows the fraction of the total intensity in the higher-frequency (defect) peak as a function of deposition temperature. For deposition temperatures below 200 K, the spectrum was too broad and indistinct to permit a meaningful separation into distinct peaks. The total integrated intensity, determined by summing the intensities of the two Lorentzians and shown in the upper portion of Fig. 5, varied by less than 10% for deposition temperatures between 200 and 400 K, indicating that the total amount of adsorbed CO at saturation did not vary significantly with deposition temperature.

It is also clear from Fig. 5 that the intensity of the defect-CO peak increases strongly with decreasing deposition temperature between 400 and about 250 K. In contrast, no visible deterioration could be seen in the LEED patterns, either of the bare surface or the  $c(2 \times 2)$  CO overlayer, for deposition temperatures above 250 K.

Because dipole coupling between the two CO species leads to intensity borrowing, the relative intensities of the two peaks cannot be directly interpreted as a measure of their

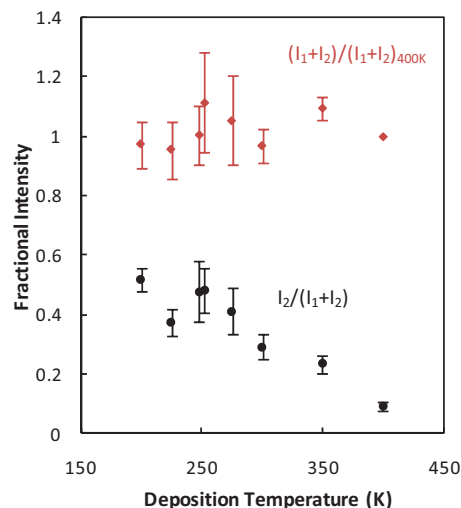


FIG. 5. Lower data set: the fraction of the total integrated intensity represented by the high-frequency (defect-site) peak as a function of sample temperature during deposition, as determined from phenomenological fitting by two Lorentzians. The error is a characteristic of the sensitivity of the decomposition to changes in the intensity parameters. Upper data set: total integrated intensity, normalized to that of the 400 K spectrum. Data points for two measurements at 250 K are slightly offset for clarity.

relative populations. To estimate defect densities from the IR spectra, we have modeled the spectra using the dipole-coupling theory of Persson and Ryberg, which has been successful in explaining the spectra of both homogeneous layers and isotopic mixtures.<sup>4</sup> Assuming that the two CO species have the same electronic and vibrational polarizabilities, the key parameters of the model are the “singleton” frequencies of the two species (i.e., the frequency for an isolated molecule, without dipole coupling)  $\nu_1$  and  $\nu_2$ , their inherent linewidths  $\gamma_1$  and  $\gamma_2$ , and the fractional concentration of the minority species  $c_2$ .

Figure 6 shows the highly nonlinear dependence of the fractional intensity in the high-frequency peak on the fractional concentration of the corresponding CO species. To generate this graph, we used fixed values of the singleton frequencies and linewidths, chosen to reproduce typical data, and computed theoretical spectra for varying values of defect

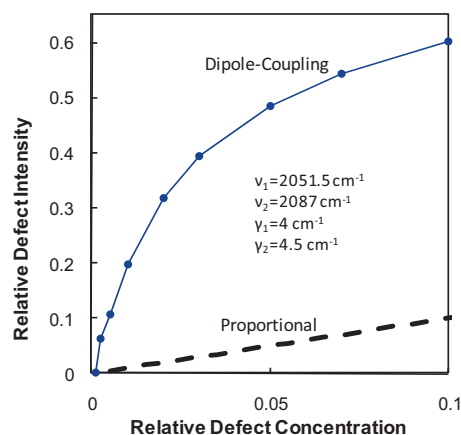


FIG. 6. Theoretical curve, based on Ref. 4, showing the highly nonlinear dependence of the defect-site intensity on defect concentration. Parameters used in the model are chosen to fit our experimental spectra. The dashed line shows the linear dependence expected in the absence of intensity borrowing.

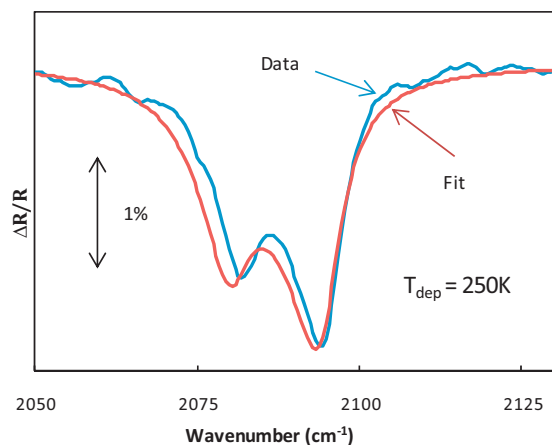


FIG. 7. Example of fit to data using the Persson–Ryberg dipole-coupling theory. Data are for saturation coverage on a Cu film deposited at 250 K. The slight deviation is due to the singleton frequency of the lower-frequency peak being held constant.

concentration  $c_2$ . These spectra were then decomposed into a sum of two Lorentzians using the same procedure that was used with the experimental data to arrive at the results in Fig. 5. At very low defect concentrations, the fractional intensity in the corresponding spectral peak increases very steeply (compared to the dashed line, which represents direct proportionality of spectral intensity to concentration). Because of this hypersensitivity to small defect concentrations, the high intensity of the feature associated with defect-bonded CO shown in Figs. 4 and 5 actually represents a much lower concentration of defect-CO.

To quantify the concentration of defect-bonded CO, we have used the Persson–Ryberg theory to fit the saturation-coverage spectrum for each deposition temperature at which two features could be distinguished, from 225 to 400 K. To reduce the number of adjustable parameters, and because we do not expect the characteristics of the terrace CO species to depend strongly on surface roughness, the singleton frequency of the terrace-CO peak was held fixed at  $2051.5 \text{ cm}^{-1}$ , and the natural linewidth of the terrace species was held fixed during fitting at a value between  $4.0$  and  $5.0 \text{ cm}^{-1}$  selected by comparison with the data. The adjust-

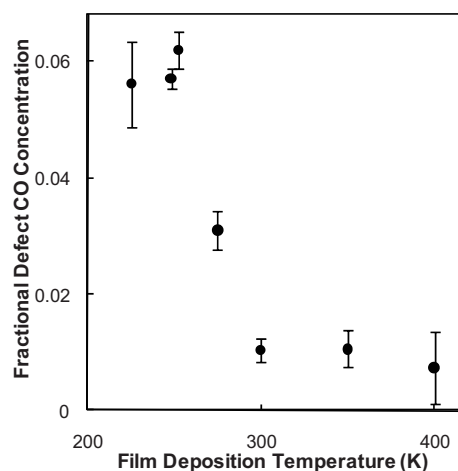


FIG. 8. Dependence of the concentration of defect-site CO on the deposition temperature of the Cu film, as determined from fitting to the dipole-coupling model (Ref. 4).

able parameters were the fractional concentration, singleton frequency, and natural linewidth of defect-bonded CO. Figure 7 shows a typical fit; even better agreement could be obtained if the terrace CO frequency and linewidth were allowed to vary freely, but even with those parameters fixed, a good match to the data is obtained. Table I lists the parameters, both fixed and free, determined from the fit for a saturation coverage of CO at each deposition temperature. The uncertainty in each parameter was estimated by manually offsetting it from its optimum value and allowing the other parameters to vary freely, until a satisfactory fit to the data could no longer be obtained. Two entirely separate measurements were carried out for a deposition temperature of 250 K. The close agreement between them is indicative of the repeatability of the experiments.

Figure 8 shows the defect-CO concentration derived from the fits to the dipole-coupling model as a function of deposition temperature. In contrast to the strong increase in the intensity of the defect-CO peak with decreasing deposition temperature shown in Fig. 5, Fig. 8 shows that the defect-CO concentration increases only very slightly as the deposition temperature decreases from 400 to 300 K, and

TABLE I. Adjustable and fixed parameters from the dipole-coupling analysis of spectra for a saturation coverage of CO on Cu films deposited at various temperatures.

Cu deposition temperature (K)	Defect CO concentration (%)	Defect CO linewidth ( $\text{cm}^{-1}$ )	Defect CO singleton frequency ( $\text{cm}^{-1}$ )
225	$5.6 \pm 0.7$	$7.4 \pm 0.4$	$2082.8 \pm 0.6$
250	$5.7 \pm 0.3$	$7.4 \pm 0.8$	$2084.4 \pm 0.3$
250	$6.2 \pm 0.2$	$7.3 \pm 0.6$	$2083.7 \pm 0.4$
275	$3.1 \pm 0.3$	$10.0 \pm 1.4$	$2087.7 \pm 0.2$
300	$1.0 \pm 0.2$	$7.5 \pm 0.3$	$2095.0 \pm 0.2$
350	$1.1 \pm 0.3$	$7 \pm 6$	$2088 \pm 7$
400	$0.7 \pm 0.6$	$7 \pm 3$	$2091 \pm 6$
Fixed parameters			
Terrace CO singleton frequency ( $\text{cm}^{-1}$ )	Terrace CO linewidth ( $\text{cm}^{-1}$ )	Electronic polarizability ( $\text{\AA}^3$ )	Vibrational polarizability ( $\text{\AA}^3$ )
2051.5	4.50	2.7	0.2



then increases sharply between 300 and 250 K. Even at deposition temperatures of 200–250 K, however, the concentration of defect-bonded CO is only about 5%–6%. It is only the disproportionately high sensitivity of the IR intensity to small concentrations of defect-bonded CO that makes it possible to observe and quantify the very low levels of surface defects at deposition temperatures between 300 and 400 K. LEED patterns remained clear and sharp for deposition temperatures as low as 250 K.

The defect concentration determined by this method appears to level off below 250 K, but, as shown in Fig. 3, the IR spectrum continues to broaden as the deposition temperature decreases to 150 K. At the lowest temperatures accessible in our experiment, we see no evidence for “re-entrant” smoothing of the surface. We cannot, of course, rule out the possibility that such smoothing occurs at temperatures below 150 K.

#### IV. CONCLUSIONS

Dipole coupling between adsorbed molecules can, under favorable conditions, greatly enhance the infrared absorption at the frequency associated with a minority species, such as defect-bonded adsorbates. This hypersensitivity is greatest when the natural vibrational frequency associated with the minority species lies slightly above that of the majority species, as in the case of terrace- and defect-bonded CO on Cu(100). We have exploited this intensity-borrowing phenomenon to characterize the surface roughness of homoepitaxial Cu films deposited on a Cu(100) crystal as a function of deposition temperature. Dipole-coupling theory was used to arrive at quantitative estimates of the defect-CO concentration.

As the deposition temperature is decreased below 400 K, the defect density increases very slightly but remains well

below 2% until the deposition temperature reaches about 300 K. Between 300 and 250 K, there is a marked increase in defect density, reaching a level of 5%–6%. There is some sign of a leveling off below 250 K, but the IR absorption spectrum becomes so broad that meaningful analysis becomes impractical. At these low temperatures, too, there is visible degradation of the LEED pattern, which is not discernible for deposition temperatures above 300 K. At the temperatures studied, down to 150 K, we see no indication of re-entrant ordering at low temperatures.

#### ACKNOWLEDGMENTS

M.H. acknowledges support from the Tufts University Summer Scholars Program. We also thank Garth Egan for his help with some of the experiments.

<sup>1</sup>G. D. Mahan and A. A. Lucas, *J. Chem. Phys.* **68**, 1344 (1978).

<sup>2</sup>M. Moskovits and J. E. Hulse, *Surf. Sci.* **78**, 397 (1978).

<sup>3</sup>M. Scheffler, *Surf. Sci.* **81**, 562 (1979).

<sup>4</sup>B. N. J. Persson and R. Ryberg, *Phys. Rev. B* **24**, 6954 (1981).

<sup>5</sup>H. Celio and M. Trenary, *Phys. Rev. Lett.* **84**, 4902 (2000).

<sup>6</sup>E. Borguet and H.-L. Dai, *J. Chem. Phys.* **101**, 9080 (1994).

<sup>7</sup>J. W. Evans, P. A. Thiel, and M. C. Bartelt, *Surf. Sci. Rep.* **61**, 1 (2006).

<sup>8</sup>D. A. Steigerwald and W. F. Egelhoff, Jr., *Surf. Sci.* **192**, L887 (1987).

<sup>9</sup>H.-J. Ernst, F. Fabre, and J. Lapujoulade, *Surf. Sci. Lett.* **275**, L682 (1992).

<sup>10</sup>H.-J. Ernst, F. Fabre, R. Folkerts, and J. Lapujoulade, *Phys. Rev. Lett.* **72**, 112 (1994).

<sup>11</sup>C. E. Botez, P. F. Miceli, and P. W. Stephens, *Phys. Rev. B* **64**, 125427 (2001).

<sup>12</sup>C. J. Hirschmugl, Y. J. Chabal, F. M. Hoffmann, and G. P. Williams, *J. Vac. Sci. Technol. A* **12**, 2229 (1994).

<sup>13</sup>F. J. Himpsel and J. E. Ortega, *Phys. Rev. B* **46**, 9719 (1992).

<sup>14</sup>M. Morin, N. J. Levinos, and A. L. Harris, *J. Chem. Phys.* **96**, 3950 (1992).

<sup>15</sup>R. Ryberg, *Phys. Rev. B* **32**, 2671 (1985).

<sup>16</sup>C. J. Hirschmugl, G. P. Williams, F. M. Hoffmann, and Y. J. Chabal, *Phys. Rev. Lett.* **65**, 480 (1990).

<sup>17</sup>J.-K. Zuo and J. F. Wendelken, *Phys. Rev. Lett.* **78**, 2791 (1997).